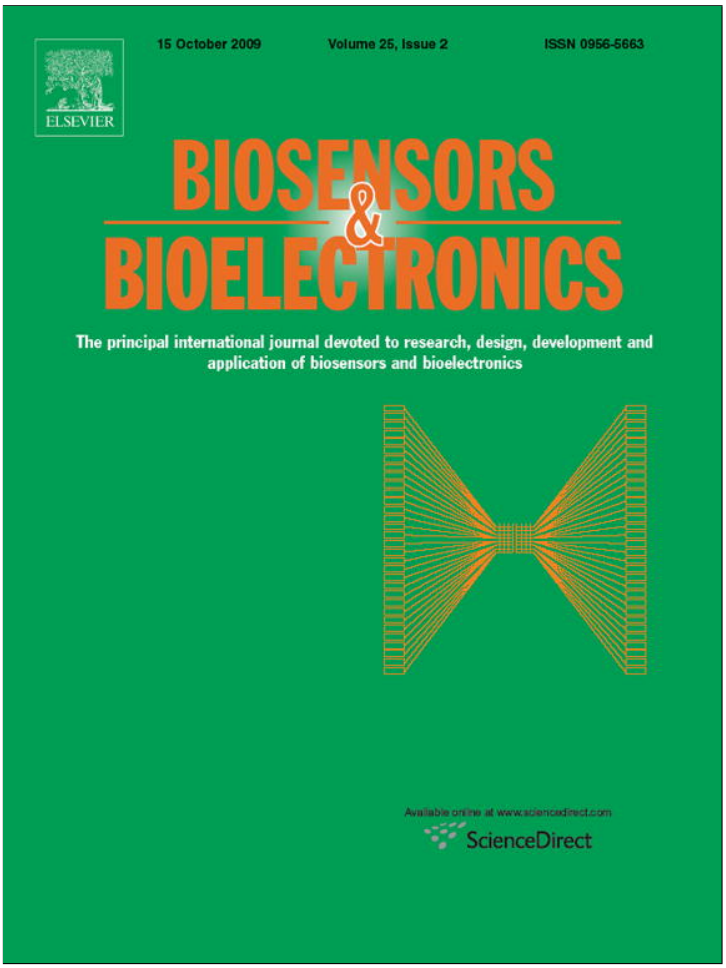

Biosensors and Bioelectronics 25 (2009) 373–377

Contents lists available at ScienceDirect

Biosensors and Bioelectronics

journal homepage: www.elsevier.com/locate/bios

A glucose biosensor based on direct electrochemistry of glucose oxidase immobilized on nitrogen-doped carbon nanotubes

Shengyuan Deng[a], Guoqiang Jian[b], Jianping Lei[a,*], Zheng Hu[b], Huangxian Ju[a,*]

[a] Key Laboratory of Analytical Chemistry for Life Science (Ministry of Education of China), Department of Chemistry, Nanjing University, Nanjing 210093, PR China
[b] Key Laboratory of Mesoscopic Chemistry (Ministry of Education of China), Department of Chemistry, Nanjing University, Nanjing 210093, PR China

ARTICLE INFO

Article history:
Received 10 May 2009
Received in revised form 3 July 2009
Accepted 21 July 2009
Available online 29 July 2009

Keywords:
Nitrogen-doped carbon nanotubes
Glucose oxidase
Direct electrochemistry
Biosensor
Biocompatibility

ABSTRACT

A novel biosensor for glucose was prepared by immobilizing glucose oxidase (GOx) on nitrogen-doped carbon nanotubes (CNx-MWNTs) modified electrode. The CNx-MWNTs membrane showed an excellent electrocatalytic activity toward the reduction of O_2 due to its diatomic side-on adsorption on CNx-MWNTs. The nitrogen doping accelerated the electron transfer from electrode surface to the immobilized GOx, leading to the direct electrochemistry of GOx. The biofunctional surface showed good biocompatibility, excellent electron-conductive network and large surface-to-volume ratio, which were characterized by scanning electron microscopy, contact angle and electrochemical impedance technique. The direct electron transfer of immobilized GOx led to stable amperometric biosensing for glucose with a linear range from 0.02 to 1.02 mM and a detection limit of 0.01 mM (S/N = 3). These results indicated that CNx-MWNTs are good candidate material for construction of the third-generation enzyme biosensors based on the direct electrochemistry of immobilized enzymes.

1. Introduction

Recently, carbon nanotubes (CNTs) have attracted great research interests in biosensing as functional material for immobilizing biomolecules and facilitating the electron transfer of redox-active sites (Katz and Willner, 2004). Due to the hydrophobicity of CNTs surface, it is necessary to functionalize CNTs with polymers, guest molecules or side wall substituents for improving the biocompatibility (Valcárcel et al., 2007). A simple way to introduce the side wall substituents on CNTs surface is oxidative functionalization. However, the complete graphene structure and relatively less defect sites on the pristine CNTs limited the introduction of the side wall substituents. Therefore, heteroatom doped carbon nanotubes, especially nitrogen-doped carbon nanotubes (CNx-MWNTs), are now extremely attractive as important nanomaterials in biosensing applications (Maldonado et al., 2006; Allen et al., 2008; Dong et al., 2008).

CNx-MWNTs usually have defective bamboo-like structure with distinctive compartment layers due to the doping of nitrogen bonded to carbon in two forms of pyridinic nitrogen and graphitic nitrogen. Compared with CNTs, CNx-MWNTs have larger surface-active groups-to-volume ratio, superb thermal stability, and good electrical and mechanical properties (Ebron et al., 2006; Gong et al., 2009). The unique physicochemical properties of CNx-MWNTs lead to extensive application in fuel cells as low-cost catalysts (Yue et al., 2008; Gong et al., 2009; Vijayaraghavan and Stevenson, 2009) and field-effect transistor devices as n-type semiconducting material (Xiao et al., 2005; Costa et al., 2008; Min et al., 2008). The less cytotoxicity and better biophilicity of CNx-MWNTs than un-doped CNTs (Carrero-Sánchez et al., 2006; Magrez et al., 2006) make them suitable to construct enzyme biosensors. Two biosensors for hydrogen peroxide and glucose have been developed based on the immobilization of horseradish peroxidase (Lyon and Stevenson, 2008) and glucose oxidase (GOx) (Jia et al., 2005) on CNx-MWNTs, respectively. The latter needed adding ferrocenemethanol in detection solution to act as a mediator for electron transfer. This work studies the electrocatalytic behaviors of CNx-MWNTs toward the reduction of both oxygen and the immobilized GOx. The excellent direct electrochemistry of GOx immobilized on CNx-MWNTs leads to a novel third-generation biosensor for glucose.

An ultimate goal of glucose sensing is to develop the third-generation biosensor (Wang, 2008), which is based on the direct electron transfer between the cofactor FAD of GOx and the electrode and can bring high selectivity without interference from monitoring the coexisted electroactive substances due to the absence of mediator. However, the direct electron transfer for oxidation of $FADH_2$ (Wang et al., 2009) or reduction of FAD (Shan et al., 2009) is hard to realize at conventional electrodes, because the FAD is deeply seated in a cavity and not easily accessible for conduction of electrons from the electrode surface. Thus, many novel nanomaterials have been explored to immobilize GOx for accelerating the electron transfer (Palmisano and Zambonin, 2002; Liu and Ju, 2003;

* Corresponding authors. Tel.: +86 25 83593593; fax: +86 25 83593593.
E-mail addresses: jpl@nju.edu.cn (J. Lei), hxju@nju.edu.cn (H. Ju).

0956-5663/$ – see front matter © 2009 Elsevier B.V. All rights reserved.
doi:10.1016/j.bios.2009.07.016

Jing and Yang, 2006; Liu et al., 2007; Wu et al., 2007c; Zhang et al., 2007b; Dai et al., 2008; Deng et al., 2008; Shan et al., 2009; Wang et al., 2009). In this work, the promoted direct electron transfer of GOx at CNx-MWNTs modified electrode and its biosensing application indicated CNx-MWNTs could be the good candidate material for immobilizing biomolecules and fabricating the third-generation biosensors.

2. Materials and methods

2.1. Materials and reagents

CNx-MWNTs with the N content of 4.6% were synthesized according to the method previously reported (Chen et al., 2006), and were further refluxed in 6 M NaOH at 110 °C for 4 h to remove the Al_2O_3 support, followed by refluxing in 1 M H_2SO_4 for 8 h to remove residual Fe catalysts (Yue et al., 2008). The purified CNx-MWNTs were thoroughly washed with double-distilled water until the pH value of the filtrate reached 7, and then dried at 70 °C overnight for further study. Multi-walled carbon nanotubes (MWCNTs) with diameter of 40–60 nm were obtained from Shenzhen Nanotech Port Company. Both nanotubes were treated by sonicating in a mixture of concentrated sulfuric acid–nitric acid (3:1, v/v) at 60 °C for 2 h. The suspension was centrifuged and washed with double-distilled water till the pH value of the filtrate reached 7. The obtained solid was redispersed in water with a concentration of 0.5 mg mL^{-1}.

GOx (EC 1.1.3.4, type X-S, lyophilized powder, 100–250 units mg^{-1}, from *Aspergillus niger*) was purchased from Sigma. D-(+)-Glucose was bought from Sinopharm Chemical Reagent Co., Ltd. Glucose stock solutions were mutarotated overnight at room temperature before use. Nafion (product No. 274704) was obtained from Aldrich. All other reagents were of analytical grade and used without further purification.

2.2. Apparatus

Electrochemical impedance measurements were carried out on a PGSTAT30/FRA2 system (Autolab, The Netherlands) in 0.1 M KCl solution containing 5 mM $K_3[Fe(CN)_6]/K_4[Fe(CN)_6]$. The electrochemical impedance spectra (EIS) were recorded in the frequency range of 10^{-2} to 10^5 Hz. The amplitude of the applied sine wave potential in each case was 5 mV. Cyclic voltammetric experiments were performed on a CHI 812B electrochemical workstation (CH Instruments Inc., USA), and differential pulse voltammetric experiments were performed on a CHI 660 electrochemical workstation (CH Instruments Inc., USA). All the electrochemical measurements were carried out in phosphate buffer solution (PBS) (0.1 M, pH 7.0) at room temperature (20 ± 2 °C) with conventional three-electrode cell consisting of a glassy carbon electrode (GCE) as working, a saturated calomel electrode (SCE) as reference and a platinum wire as counter electrodes.

After coated with Au film to improve the conductivity, the sample films were examined under a Hitachi S-4800 scanning electron microscope (Hitachi, Japan). The static water contact angles were measured at 20 °C by a contact angle meter (Rame-Hart-100) employing drops of pure deionized water.

2.3. Preparation of GOx/CNx-MWNTs modified GCE

The GCE was successively polished to a mirror finish using 0.3 and 0.05 μm alumina slurry (Beuhler) followed by rinsing thoroughly with double-distilled water. After successive sonication in ethanol and double-distilled water, the electrode was rinsed with double-distilled water and allowed to dry at room temperature. 3.5 μL of CNx-MWNTs suspension was dropped on the pretreated GCE surface and dried at room temperature to form CNx-MWNTs modified GCE. Then CNx-MWNTs modified GCE was immersed into 0.1 M PBS containing 2 mg mL^{-1} GOx for 20 h at 4 °C in refrigerator. The resulting GOx/CNx-MWNTs modified GCE was then rinsed throughout with double-distilled water to wash away the loosely adsorbed enzyme molecules. To maintain the stability of modified GCE, a drop of 4.0 μL 1% Nafion solution was cast on the membrane before electrochemical measurements. For comparison, GOx/MWCNTs modified GCE and GOx modified GCE were also prepared with the same procedure. All enzyme-modified electrodes were stored in 0.1 M pH 7.0 PBS at 4 °C in refrigerator when not in use.

3. Results and discussion

3.1. Characterization of GOx/CNx-MWNTs modified GCE

The scanning electron micrograph (SEM) of CNx-MWNTs film displayed a well-dispersed one-dimensional structure with the outer diameter from 40 to 60 nm (Inset of photo a, Fig. 1A). This uniform and interdigitated nanostructure provided a significant increase of effective area for protein loading. When GOx solution was cast on CNx-MWNTs film (photo b, Fig. 1A), the GOx molecules adsorbed on the surface of CNx-MWNTs and tended to aggregate into island-like structures. The open structure of GOx/CNx-MWNTs film facilitated the substrate accessible to GOx and resulted in good electrochemical response to glucose.

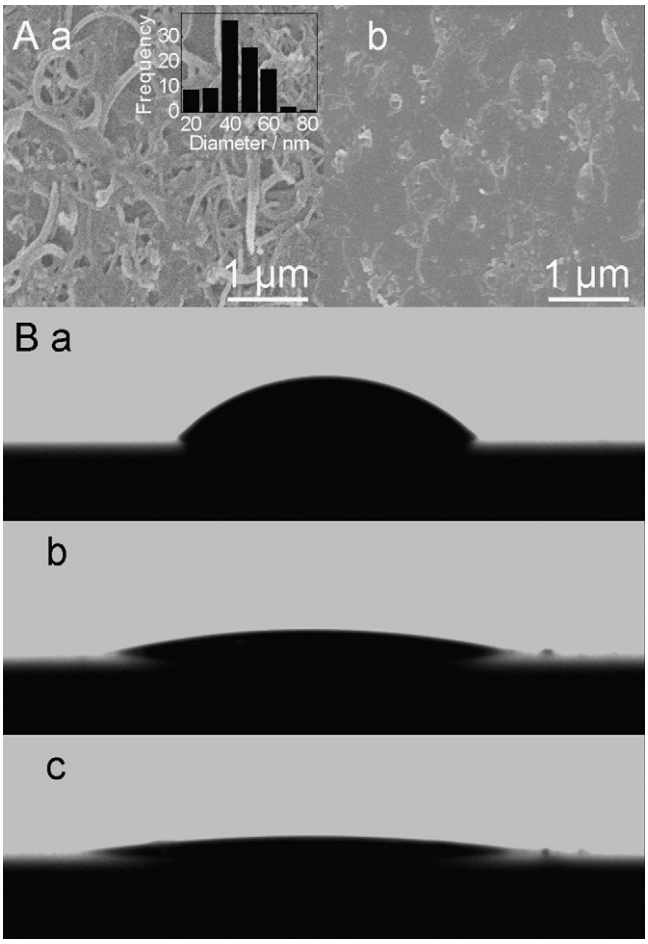

Fig. 1. (A) Scanning electron micrographs of (a) CNx-MWNTs and (b) GOx/CNx-MWNTs films. Inset: diameter distribution of CNx-MWNTs. (B) Contact angles of (a) bare, (b) MWCNTs and (c) CNx-MWNTs modified substrates.

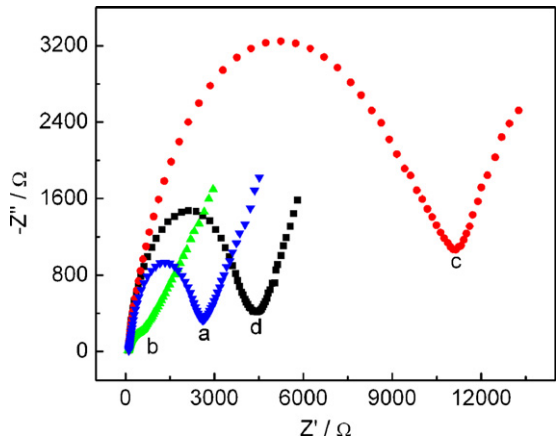

Fig. 2. Electrochemical impedance spectra of (a) bare, (b) CNx-MWNTs, (c) GOx, and (d) GOx/CNx-MWNTs modified GCEs in 0.1 M KCl solution containing 5 mM $K_3[Fe(CN)_6]/K_4[Fe(CN)_6]$.

The biocompatibility of an interface can be characterized by its hydrophilicity, which can be qualitative by measuring the contact angle of the substrate (Wu et al., 2007b). The contact angles of the bare glass slide, MWCNTs and CNx-MWNTs film were measured to be 44°, 15° and 8°, respectively (Fig. 1B). The lower contact angle of CNx-MWNTs film than MWCNTs film indicated better hydrophilicity, which could be contributed to the multiple defects from nitrogen doping and more hydrophilic groups produced by acidic treatment (Burch et al., 2008). The improved biocompatibility of CNx-MWNTs could greatly enhance the loading capacity of protein and preserve the bioactivity of the immobilized biomolecules.

By using $K_3[Fe(CN)_6]/K_4[Fe(CN)_6]$ redox couple as an electrochemical probe, the Nyquist plots of different electrodes in the frequency range from 10^{-2} to 10^5 Hz were obtained (Fig. 2). At a bare GCE the redox process of the probe showed an electron-transfer resistance of about 2800 Ω (curve a), which was much larger than that of CNx-MWNTs modified GCE (curve b), indicating CNx-MWNTs could act as a good electron-transfer interface between the EIS probe and the electrode. After GOx was coated on the bare electrode, the resistance increased dramatically to about 10^5 Ω (curve c), suggesting that the bulky GOx molecules blocked the electron exchange between the redox probe and electrode surface. When GOx was adsorbed on CNx-MWNTs modified GCE, the semicircle diameter in Nyquist plot was much lower than that of GOx modified GCE (curve d), indicating that the presence of CNx-MWNTs enhanced the electron transfer of the redox probe, which could also accelerate the electron transfer between the electroactive sites embedded in enzymes and the electrode.

3.2. Electrocatalysis of O_2 reduction at CNx-MWNTs modified GCE

Fig. 3 shows the cyclic voltammograms of MWCNTs and CNx-MWNTs modified GCE in 0.1 M PBS at 100 mV s^{-1}. In nitrogen-saturated PBS, both the CNTs modified GCE showed one pair of redox peaks at −0.03 and −0.18 V, which could be ascribed to the oxidation and reduction of the oxygen-containing groups produced by the acid-treatment (Wu et al., 2007a). The peak currents at CNx-MWNTs modified GCE was 2.2 times larger than those of MWCNTs modified GCE (Fig. 3a), suggesting more defects on CNx-MWNTs to form more oxygen-containing groups (Burch et al., 2008), which were favorable to improving the biocompatibility for protein immobilization and enhancing the electrocatalytic activity of CNTs toward the reduction of both O_2 and the immobilized electroactive enzymes.

As expected, the CNx-MWNTs exhibited better electrocatalysis toward the reduction of O_2 than MWCNTs (Fig. 3b and c). In air-saturated PBS an obvious reduction peak of O_2 at CNx-MWNTs modified GCE could be observed at −0.16 V, while the peak at MWCNTs modified GCE occurred at −0.59 V. The corresponding peak current densities were 0.145 and 0.128 mA cm^{-2}, respectively. In oxygen-saturated PBS the difference in peak current density was more obvious. It was 1.76 times larger than that at MWCNTs modified GCE. Additionally, when 1.0 mM H_2O_2 was added in nitrogen-saturated PBS at CNx-MWNTs modified GCE, the CV curves have no obvious difference in the potential range from −0.8 to +0.8 V (not shown), indicating the catalysts could be removed after purification and acid-treatment steps, and the electrochemical reactivity toward the oxygen could not be attributed to the presence of catalysts. The better electrocatalysis was due to the more oxygen-containing groups and the nitrogen-induced charge delocalization at CNx-MWNTs. The latter changed the chemisorption mode of O_2 from the usual monoatomic end-on adsorption at MWCNTs to a diatomic side-on adsorption at CNx-MWNTs, which could effectively weaken the O–O bonding to facilitate the reduction of O_2 (Gong et al., 2009). The sensitive response of the CNx-MWNTs to O_2 could be further developed for detection of dissolved oxygen.

3.3. Direct electrochemistry of GOx/CNx-MWNTs modified GCE

The direct electrochemistry of GOx immobilized on CNx-MWNTs modified GCE was investigated in 0.1 M nitrogen-saturated PBS. The cyclic voltammogram of GOx/CNx-MWNTs modified GCE at 100 mV s^{-1} showed a pair of well-defined redox peaks at −0.446 and −0.473 V (Fig. 4a), while the GOx modified GCE did not show any response (Fig. 4b). Obviously, the presence of CNx-MWNTs resulted in the direct electrochemistry of GOx. The peak potential separation of 27 mV at GOx/CNx-MWNTs modified GCE was

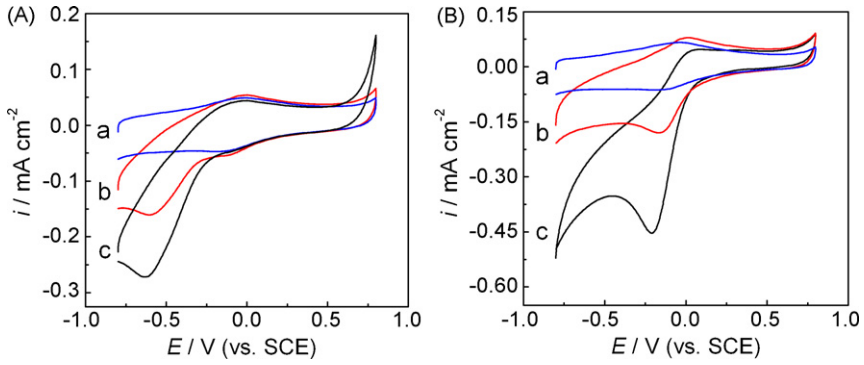

Fig. 3. Cyclic voltammograms of (A) MWCNTs and (B) CNx-MWNTs modified GCEs in (a) nitrogen-saturated, (b) air-saturated and (c) oxygen-saturated 0.1 M pH 7.0 PBS. Scan rate: 100 mV s^{-1}.

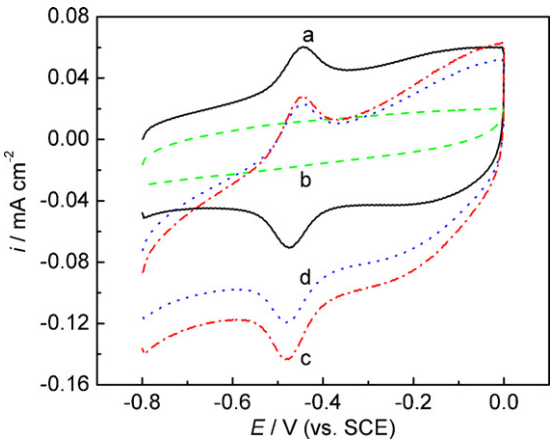

Fig. 4. Cyclic voltammograms of (a) GOx/CNx-MWNTs and (b) GOx modified GCEs in nitrogen-saturated 0.1 M pH 7.0 PBS, and GOx/CNx-MWNTs in air-saturated 0.1 M pH 7.0 PBS in the (c) absence and (d) presence of 1.0 mM glucose. Scan rate: 100 mV s^{-1}.

much smaller than that of 95 mV at GOx/Au nanoparticles/carbon paste electrode (Liu and Ju, 2003), indicating the faster direct electron transfer between the redox-active site of GOx (the cofactor FAD) and GCE without the help of electron transfer mediator. The anodic and cathodic peak currents linearly increased with the increasing scan rate from 10 to 450 mV s^{-1} (Fig. 5), indicating a surface-controlled process. From the peak potential separation, the apparent electron transfer rate constant (k_s) was estimated to be 4.6 s^{-1} (Laviron, 1979), which was lager than those of 3.13 s^{-1} at GOx/MWCNTs, 1.56 s^{-1} at boron-doped CNTs (Deng et al., 2008), and 3.3 s^{-1} at single-walled CNTs (Zhang et al., 2007b) modified GCE. This result further proved that CNx-MWNTs facilitated the electron transfer between redox-active sites of enzyme and the electrode.

The amount of electroactive GOx adsorbed on the electrode surface could be evaluated from the charge integral of the cathodic peak in curve a. The value was estimated to be 7.52×10^{-10} mol cm^{-2}, which was higher than those of 5.88×10^{-10} mol cm^{-2} at MWCNTs modified GCE, 9.8×10^{-12} mol cm^{-2} at GOx/Au nanoparticles/carbon paste electrode (Liu and Ju, 2003), 1.54×10^{-11} mol cm^{-2} at GOx/CdS modified electrode (Huang et al., 2005) and 2.86×10^{-12} mol cm^{-2} at bare GCE (Zhang et al., 2007a). These results confirmed that CNx-MWNTs modified electrode was advantageous for the direct electron transfer of GOx because of the excellent conductivity and large capacity for protein loading.

With the increasing pH from 5.0 to 9.0, the redox potentials of GOx/CNx-MWNTs modified GCE shifted linearly to more negative values with a slope of −58.4 mV pH^{-1} for the reduction process. The slope was close to the theoretical value of −58.6 mV pH^{-1} at 20 °C, indicating a two-proton participated two-electron redox process.

3.4. Detection of glucose based on direct electrochemistry at GOx/CNx-MWNTs modified GCE

In air-saturated PBS, the cyclic voltammogram of GOx/CNx-MWNTs showed greatly increased reduction peak current (curve c, Fig. 4), while the oxidation peak current decreased, showing an obvious electrocatalytic process toward the reduction of dissolved oxygen according to the following equations (Liu and Ju, 2003):

$$\mathrm{GOx\ (FAD)} + 2e^- + 2H^+ \rightleftharpoons \mathrm{GOx\ (FADH_2)} \quad (1)$$

$$\mathrm{GOx\ (FADH_2)} + O_2 \rightarrow \mathrm{GOx\ (FAD)} + H_2O_2 \quad (2)$$

This was a typical EC catalytic process (Bard and Faulkner, 2001), in which oxygen regenerated GOx (FAD) and enhanced the reduction peak current of FAD. When glucose was added into this system, the reduction peak current decreased (curve d, Fig. 4). Thus the glucose restrained the electrocatalytic reaction due to the enzyme-catalyzed reaction between the oxidized form of GOx, GOx (FAD), and glucose, which diminished the concentration of the GOx (FAD) as shown in Eq. (3):

$$\mathrm{Glucose + GOx\ (FAD) \rightarrow Gluconolactone + GOx\ (FADH_2)} \quad (3)$$

With the increasing glucose concentration, the peak current for the electrocatalytic reduction decreased, producing a glucose biosensor.

Fig. 6 shows the differential pulse voltammetric measurements using GOx/CNx-MWNTs modified GCE in air-saturated 0.1 M pH 7.0 PBS upon addition of glucose. The relatively large peak at −0.5 V was ascribed to the reduction of FAD, while the small peak near −0.16 V could be considered to be the reduction of oxygen-containing groups on CNx-MWNTs. The peak current of GOx/CNx-MWCNTs modified GCE decreased linearly with the increasing concentration of glucose up to 1.02 mM with a detection limit of 0.01 mM (S/N = 3). Furthermore, the sensitivity of GOx/CNx-MWNTs modified GCE was calculated to be 13.0 μA mM^{-1} cm^{-2}, which was higher than

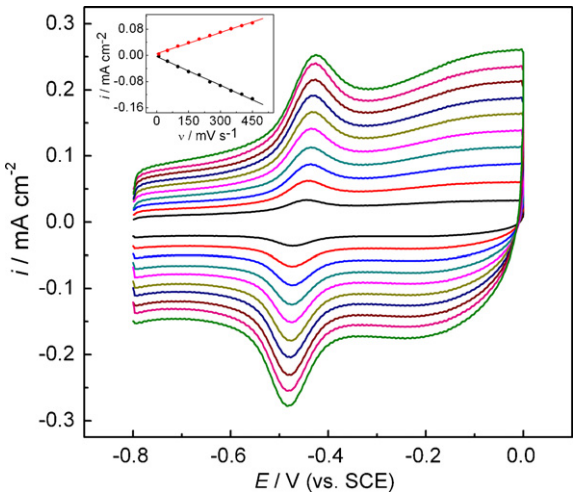

Fig. 5. Cyclic voltammograms of GOx/CNx-MWNTs modified GCE in nitrogen-saturated 0.1 M pH 7.0 PBS. Inset: plots of (a) cathodic and (b) anodic peak currents *vs.* scan rate.

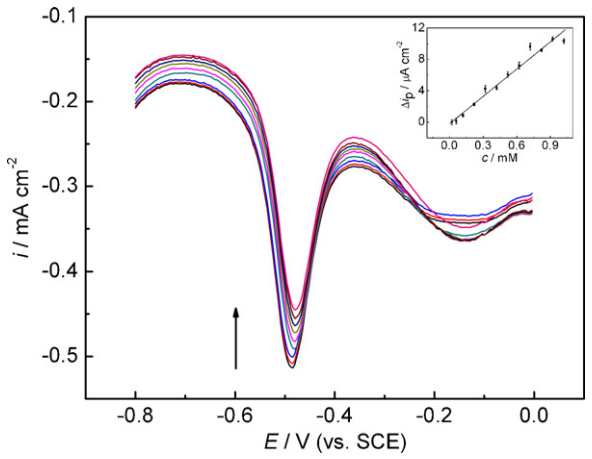

Fig. 6. Differential pulse voltammograms of GOx/CNx-MWNTs modified GCE in air-saturated 0.1 M pH 7.0 PBS containing 0, 0.02, 0.05, 0.12, 0.32, 0.52, 0.72, 0.92 and 1.02 mM glucose (from bottom to top). Inset: calibration curve at a pulse amplitude of 50 mV and a pulse width of 50 ms.

0.2, 1.06 and 0.053 μA mM^{-1} cm^{-2} for the glucose biosensors based on MWCNTs (Salimi et al., 2004), single-walled carbon nanohorns (Liu et al., 2008) and highly ordered mesoporous carbon foams (Zhou et al., 2008).

The apparent Michalis–Menten constant (K_m^{app}), an indicator of enzyme-substrate reaction kinetics, can be used to evaluate the biological activity of the immobilized enzyme. Here, the K_m^{app} value of GOx/CNx-MWNTs modified GCE was estimated to be 2.2 mM, which was smaller than those of 14.4, 21 and 37.6 mM for immobilized GOx (Zheng et al., 2002; Chen et al., 2003; Uang and Chou, 2003), indicating that the GOx immobilized on CNx-MWNTs had high affinity to glucose.

The effect of possible interfering species on glucose detection was examined using 1.00 mM uric acid or ascorbic acid, which caused an increase of 3.4% or 4.7% in the reduction current of 0.10 mM glucose, respectively. This result suggested that the proposed glucose had high selectivity, and no interference from those endogenously coexisted electroactive substances (Wolfrum et al., 2008) due to the low operating potential.

The analysis of glucose was carried out in serum without any need of sample pretreatment except a dilution step. The concentration of glucose in a serum sample was determined to be 4.45 mM, which was consistent with the value of 4.58 mM obtained by spectrophotometry. The recovery tests were performed by adding 0.10 and 0.50 mM glucose to the serum sample, which produced the recovery of 104 ± 5.7% and 94 ± 6.6%, demonstrating good accuracy for the determination of glucose in real samples.

The reproducibility of the glucose biosensor was investigated by successively detecting 0.10 mM glucose for 10 times, the relative standard deviation (RSD) was 5.0%, demonstrating a good reproducibility. After 40 successively scanning the response was still retained 95% value of the initial response, suggesting the acceptable durability of the biosensors. In addition, the RSD of current signals for measurement of 0.10 mM glucose at five independently prepared biosensors was 3.9%, which proved good reproducibility of the biosensor preparation.

When stored in 0.1 M pH 7.0 PBS at 4 °C and measured at intervals over several days, no obvious decrease in the response to glucose was observed after one week of storage. After 20 days the response was still retained 96% value of the initial response. This implied that the GOx/CNx-MWNTs modified GCE was very efficient for retaining the bioactivity of enzyme and preventing its leakage from the membrane.

4. Conclusions

A third-generation glucose biosensor is developed based on the direct electrochemistry of glucose oxidase immobilized on nitrogen-doped carbon nanotubes. The CNx-MWNTs exhibit excellent biocompatibility, high conductivity and good electrocatalysis toward the reduction of O_2, provide a significantly increased effective area for protein loading, and accelerate the electron transfer between the electroactive sites embedded in protein and the electrode. The direct electrochemistry of glucose oxidase is a two-proton participated two-electron redox process. Based on the restraint of glucose to the electrocatalytic process of GOx/CNx-MWNTs toward the reduction of dissolved oxygen, the proposed biosensor shows sensitive amperometric biosensing for glucose with a linear range from 0.02 to 1.02 mM and a detection limit of 0.01 mM (S/N = 3), high affinity, excellent selectivity, acceptable reproducibility and stability. It has been used for detection of glucose in real sample with good accuracy. CNx-MWNTs would serve as an excellent material for construction of the third-generation enzyme biosensors.

Acknowledgments

This research was financially supported by the National Science Funds for Creative Research Groups (20821063), Major Research Plan (90713015), and the projects (20535010, 20705012 and 20875044) from the National Natural Science Foundation of China, and One Specific Program for Creative Scholars (BK2008014) from the Natural Science Foundation of Jiangsu Province.

References

Allen, B.L., Kichambare, P.D., Star, A., 2008. ACS Nano 9, 1914–1920.
Bard, A.J., Faulkner, L.R., 2001. Electrochemical Methods: Fundamentals and Applications, 3rd ed. John Wiley & Sons, Inc., New York.
Burch, H.J., Contera, S.A., de Planque, M.R.R., Grobert, N., Ryan, J.F., 2008. Nanotechnology 19, 384001.
Carrero-Sánchez, J.C., Elías, A.L., Mancilla, R., Arrellín, G., Terrones, H., Laclette, J.P., Terrones, M., 2006. Nano Lett. 8, 1609–1616.
Chen, H., Yang, Y., Hu, Z., Huo, K.F., Ma, Y.W., Chen, Y., 2006. J. Phys. Chem. B 110, 16422–16427.
Chen, X., Jia, J., Dong, S., 2003. Electroanalysis 15, 608–612.
Costa, P.M.F.J., Golberg, D., Mitome, M., Bando, Y., 2008. Appl. Phys. A 90, 225–229.
Dai, Z.H., Bao, J.C., Yang, X.D., Ju, H.X., 2008. Biosens. Bioelectron. 23, 1070–1076.
Deng, C.Y., Chen, J.H., Chen, X.L., Xiao, C.H., Nie, L.H., Yao, S.Z., 2008. Biosens. Bioelectron. 23, 1272–1277.
Dong, J.P., Qu, X.M., Wang, L.J., Zhao, C.J., Xua, J.Q., 2008. Electroanalysis 18, 1981–1986.
Ebron, V.H., Yang, Z.W., Seyer, D.J., 2006. Science 311, 1580–1583.
Gong, K.P., Du, F., Xia, Z.H., Durstock, M., Da, L.M., 2009. Science 323, 760–764.
Huang, Y.X., Zhang, W.J., Xiao, H., Li, G.X., 2005. Biosens. Bioelectron. 21, 817–821.
Jia, N.Q., Liu, L., Zhou, Q., Wang, L.J., Yan, M.M., Jiang, Z.Y., 2005. Electrochim. Acta 51, 611–618.
Jing, W., Yang, Q., 2006. Anal. Bioanal. Chem. 385, 1330–1335.
Katz, E., Willner, I., 2004. ChemPhysChem 5, 1084–1104.
Laviron, E., 1979. J. Electroanal. Chem. 101, 19–28.
Liu, S.Q., Ju, H.X., 2003. Biosens. Bioelectron. 19, 177–183.
Liu, G.Z., Paddon-Row, M.N., Gooding, J.J., 2007. Electrochem. Commun. 9, 2218–2223.
Liu, X., Shi, L., Niu, W., Li, H., Xu, G., 2008. Biosens. Bioelectron. 23, 1887–1890.
Lyon, J.L., Stevenson, K.J., 2008. Electrochim. Acta 53, 6714–6721.
Magrez, A., Kasas, S., Salicio, V., Pasquier, N., Seo, J.W., Celio, M., Catsicas, S., Schwaller, B., Forró, L., 2006. Nano Lett. 6, 1121–1125.
Maldonado, S., Morin, S., Stevenson, K.J., 2006. Analyst 131, 262–267.
Min, Y.S., Bae, E.J., Kim, U.J., Lee, E.H., Park, N.J., Hwang, C.S., Park, W.J., 2008. Appl. Phys. Lett. 93, 043113.
Palmisano, F., Zambonin, P.G., 2002. Anal. Chem. 74, 5913–5918.
Salimi, A., Compton, R.G., Hallaj, R., 2004. Anal. Biochem. 333, 49–56.
Shan, C.S., Yang, H.F., Song, J.F., Han, D.X., Ivaska, A., Niu, L., 2009. Anal. Chem. 81, 2378–2382.
Uang, Y., Chou, T.C., 2003. Biosens. Bioelectron. 20, 2435–2453.
Valcárcel, M., Cárdenas, S., Simonet, B.M., 2007. Anal. Chem. 79, 4788–4797.
Vijayaraghavan, G., Stevenson, K.J., 2009. Langmuir 23, 5279–5282.
Wang, J., 2008. Chem. Rev. 108, 814–825.
Wang, Z.Y., Liu, S.N., Wu, P., Cai, C.X., 2009. Anal. Chem. 81, 1638–1645.
Wolfrum, B., Zevenbergen, M., Lemay, S., 2008. Anal. Chem. 80, 972–977.
Wu, L.N., Zhang, X.J., Ju, H.X., 2007a. Analyst 132, 406–408.
Wu, L.N., Zhang, X.J., Ju, H.X., 2007b. Anal. Chem. 79, 453–458.
Wu, S., Ju, H.X., Liu, Y., 2007c. Adv. Funct. Mater. 17, 585–592.
Xiao, K., Liu, Y.Q., Hu, P.A., Yu, G., Sun, Y.M., Zhu, D.B., 2005. J. Am. Chem. Soc. 24, 8614–8617.
Yue, B., Ma, Y.W., Tao, H.S., Yu, L.S., Jian, G.Q., Wang, X.Z., Wang, X.S., Lu, Y.N., Hu, Z., 2008. J. Mater. Chem. 18, 1–5.
Zhang, J.D., Feng, M.L., Tachikawa, H., 2007a. Biosens. Bioelectron. 22, 3036–3041.
Zhang, Y.J., Han, D.X., Wang, Z.J., Song, J.X., Niu, L., 2007b. Biosens. Bioelectron. 23, 438–443.
Zheng, H., Xue, H., Zhang, Y., Shen, Z., 2002. Biosens. Bioelectron. 17, 541–545.
Zhou, M., Shang, L., Li, B., Huang, L., Dong, S., 2008. Biosens. Bioelectron. 24, 442–447.